SUPPLEMENTARY MATERIALS

Allometry of antipredatory jumping on water by water striders

Woojoo Kim[1&], Juliette Amauger[2&], Jungmoon Ha[1], Thai Pham Hong[3,4], Anh Duc Tran[5], Jae Hong Lee[6], Jinseok Park[1], Piotr G. Jablonski[1,7*], Ho-Young Kim[6*], Sang-im Lee[8*]

Affiliations:

[1] Laboratory of Behavioral Ecology and Evolution, School of Biological Sciences, Seoul National University, Seoul 08826, Korea
[2] LadHyX, UMR 7646 du CNRS, École Polytechnique, 91128 Palaiseau, France
[3] Mientrung Institute for Scientific Research (MISR), Vietnam National Museum of Nature, Vietnam Academy of Science and Technology (VAST), 321 Huynh Thuc Khang St, Hue, Vietnam
[4] Graduate University of Science and Technology, VAST, 18 Hoang Quoc Viet, Cau Giay, Hanoi, Vietnam
[5] Department of Applied Zoology, Faculty of Biology, University of Science, Vietnam National University, Hanoi, 334 Nguyen Trai, Thanh Xuan, Hanoi, Vietnam
[6] Department of Mechanical Engineering, Seoul National University, Seoul 08826, Korea
[7] Museum and Institute of Zoology, Polish Academy of Sciences, Wilcza 64, 00-679 Warsaw, Poland
[8] Laboratory of Integrative Animal Ecology, Department of New Biology, DGIST, Korea

*Correspondence to (alphabetically): piotrjab@behecolpiotrsangim.org (P. G. J.), hyk@snu.ac.kr (H.-Y. K.), and sangim@dgist.ac.kr (S.-i.L.)

[&] these authors equally contributed to the work

Contents

Supplementary Materials PART 1. Morphology of the study species: *Gigantometra gigas*, *Ptilomera tigrina* and *Aquarius paludum*.

In 2015, After 3-4 days of intensive searching for *G. gigas* in the creeks within the easily accessible parts of the Pu Mat National Park and surrounding area, we finally discovered one location with a small population of *G. gigas* in a creek located in a rectangular area within *18.984555, 104.782765 and 18.946744, 104.857936* (Google map coordinates; corresponding to *18°59'04.4"N 104°46'58.0"E* and *18°56'48.3"N 104°51'28.6"E* respectively). We purposely do not give the exact GPS location to prevent collectors from exploitation of this small population. We visited the population twice for a very short period each time, in 2015 and in 2018. We conducted observations and experiments directly at the field site. In 2018 the population was diminished due to the destruction of their habitat by human activities; construction of a new forest road and a use of the stream bed by motorcyclists (an occasionally probably cars) travelling into the forested area. Hence, it seems that this population is endangered and may disappear due to further anthropogenic developments because it is located outside of the strictly protected National Park borders.

Table S1. Morphology of the giant water striders, *Gigantometra gigas*, from the study site in Pu Mat National Park, Vietnam.

Variable	Males	Females
Sample size (nr of individuals)	16	9
Mass (mean ± SD, min-max; mg)	414 ± 59, 316-511	265 ± 40, 217-318
Body length (cm)	3.52 ± 0.20	3.39 ± 0.32
FRONT LEGS:		
Tibia Thickness (mm)	0.41 ± 0.05	0.39 ± 0.04
Femur length (cm)	1.11 ± 0.10	1.00 ± 0.10
Tibia length (cm)	0.89 ± 0.07	0.75 ± 0.06
Tarsus length (cm)	0.27 ± 0.03	0.23 ± 0.03
Total leg length (cm)	2.27 ± 0.17	1.99 ± 0.15
MIDLEGS:		
Tibia Thickness (mm)	0.46 ± 0.08	0.39 ± 0.04
Femur length (cm)	4.84 ± 0.45	3.32 ± 0.28
Maximum wetted leg length (Tibia + tarsus length; cm)	5.35 ± 0.60	3.85 ± 0.24
Total leg length (cm)	10.19 ± 1.04	7.17 ± 0.43
HINDLEGS:		
Tibia Thickness (mm)	0.56 ± 0.09	0.40 ± 0.05
Femur length (cm)	4.95 ± 0.69	3.21 ± 0.11
Maximum wetted leg length (Tibia + tarsus length; cm)	7.35 ± 1.16	4.06 ± 0.50
Total leg length (cm)	12.30 ± 1.25	7.26 ± 0.57

Table S2. Morphology of the three individuals for whom the jumps were fully analyzed. Thickness of the tibia was measured near the femur/tibia joint as a diameter of leg measured along horizontal line (parallel to water surface in normal position of a leg of a water strider standing on the water surface). The thickness is used in the model to calculate drag force after correction for the presence of air bubble that forms air sheath around the leg moving in the water (see calculations in Supplementary Materials PART 7)

Clip name	Mass (mg)	Middle leg			Hind leg	
		Basal Tibia Thickness (mm)	Femur length (cm)	Constant wetted length: *tibia* + *tarsus* (cm)	Femur length (cm)	Constant wetted length *tibia* + *tarsus* (cm)
EVT16	483	0.455	4.809	5.460	4.742	7.948
EVT05 (2)	375	0.390	4.286	4.578	4.274	6.336
EVT41	325	0.475	4.913	5.405	4.824	7.717

Table S3. Morphology of *Ptilomera tigrina* from two study sites: the Melinh Station for Biodiversity, Vinh Phuc Province, Vietnam, and at the "May waterfalls" (Thac May) of the Cuc Phuong National Park, Vietnam; and morphology of *Aquarius paludum* females from South Korea, Seoul.

Variable	***Ptilomera tigrina***	***Aquarius paludum***
Sample size (nr of individuals)	18	8
Mass (mean ± SD, min-max; mg)	115 ± 22, 83-144	48 ± 4, 43-54
Body length (cm)	1.72 ± 0.08	1.55 ± 0.06
MIDLEGS:		
Tibia Thickness (mm)	0.31 ± 0.03	0.18 ± 0.02
Femur length (cm)	2.40 ± 0.16	1.15 ± 0.10
Maximum wetted leg length (Tibia + tarsus length; cm)	2.39 ± 0.16	1.34 ± 0.07
Total leg length (cm)	4.79 ± 0.30	2.50 ± 0.16
HINDLEGS:		
Femur length (cm)	2.76 ± 0.23	1.21 ± 0.08
Maximum wetted leg length (Tibia + tarsus length; cm)	1.91 ± 0.19	0.95 ± 0.07
Total leg length (cm)	4.66 ± 0.42	2.16 ± 0.14

Table S4. The midleg downward stroke, L_m, the dimensionless angular velocity of middle leg rotation of a jump, Ω_m, and the dimensionless index of insect body mass with respect to the middle leg, M_m, were calculated according to the following formula from Yang et al.[1], but modified to focus on midleg, as $L_m = \Delta l_l / l_c$, $\Omega_\mathrm{m} = \omega_e (l_c/g)^{1/2}$, $M_m = m/(\rho l_c^2 C_{m0} l_m)$, because we observed that hindleg does not penetrate the water surface (see details in Supplementary Material PART 8 and Model description.pdf). The summary of these data is shown in Fig. 6

Parameter/variable (unit)	*G. gigas* male			*G. gigas* female			*P. tigrina*			*A. paludum* female		
	EVT05 (2)	EVT16	EVT41	EVT28	EVT33	EVT35	C0046	C0049	C0066	P_Female_evt25	P_Female_evt32	P_Female_evt33
m (kg)	374.76e-6	483.23e-6	325.41e-6	305.67e-6	226.81e-6	226.81e-6	134e-6	134e-6	123e-6	48.5e-06	42.6e-06	42.6e-06
y_i (m)	0.00017	0.00165	0.00088	0.00333	0.00435	0.00274	0.00271	0.00473	0.00806	0.00271	0.00473	0.00806
l_l (m)	88.64e-3	102.69e-3	103.17e-3	72.59e-3	70.13e-3	70.13e-3	44.72e-3	44.72e-3	50.63e-3	0.02434	0.02413	0.02413
l_m (m)	45.78e-3	54.60e-3	54.05e-3	39.80e-3	38.87e-3	38.87e-3	22.70e-3	22.70e-3	25.56e-3	13.56e-3	13.06e-3	13.06e-3
ω_e	20	15	16	16	19	17	41	33	29	39	40	41
L_m	32.604	37.240	37.701	25.527	24.240	24.836	15.481	14.740	15.688	7.970	7.151	5.921
Ω_m	0.333	0.250	0.266	0.266	0.316	0.283	0.682	0.549	0.483	0.649	0.666	0.682
M_m	3.029	3.369	2.169	2.388	1.993	1.993	1.624	1.624	1.190	0.874	0.696	0.696
$\Omega_\mathrm{m} M_m^{1/2}$	0.579	0.458	0.392	0.411	0.446	0.399	0.869	0.700	0.526	0.607	0.555	0.569

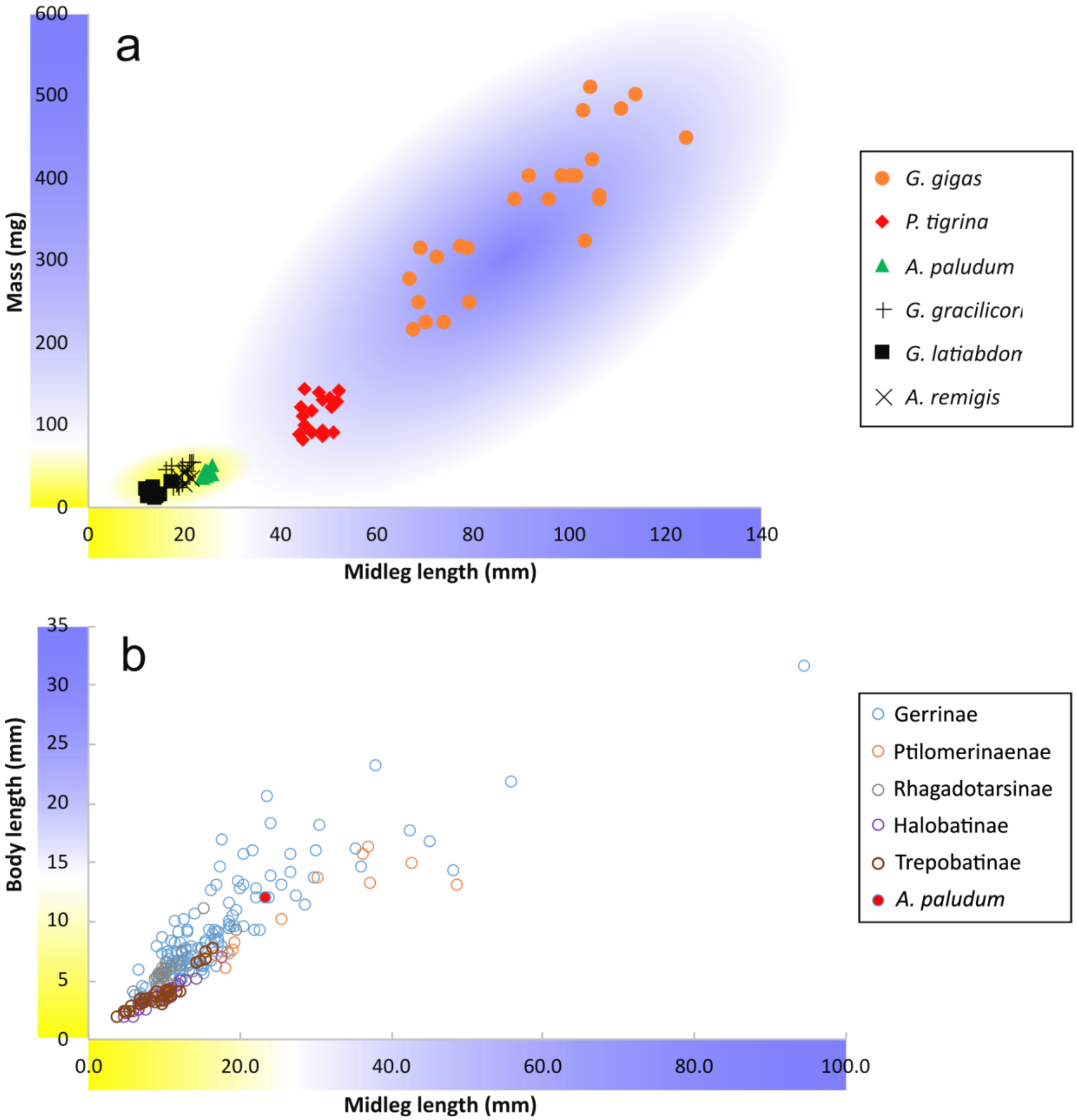

Fig. S1. Relationship between body size and midleg length in the previously studied (yellow ranges on axes) and the unstudied (blue ranges on axes) species of Gerridae divided into 5 subfamilies. a) the absolute midleg length (mm; the variable crucial for empirical biologists and directly related to the dimensionless downward stroke "L", the key variable crucial in the theoretical hydrodynamic model of jumping and shown on the horizontal axis in Fig. 1) and the species body mass (empirical variable related to the dimensionless body mass, *M*, contributing to the index of angular velocity of midleg rotation, $\Omega M^{1/2}$, which is the key variable the theoretical hydrodynamic model of jumping and is shown on the vertical axis in Fig. 1) for several species from the "typical" water striders (measured in this study: *Gerris latiabdominis, G. gracilicornis, Aquarius remigis, A. paludum*), and from the two large species that have rarely been studied before and were measured here (*Ptilomera tigrina* and *Gigantometra gigas*). b) Reconstructed data from Table 16 in Matsuda 1960[1]. Matsuda states the unit converting rule on page 32: "In table 16, 82 units are equal to 10 mm. For those values with asterisks, 173.7 units are equal to 10 mm.". However, in comparison with our measurement data, the rule seems clearly a mistake. Therefore, we used converting rule of '173.7 units are equal to 10 mm', which lead to results consistent with our data in leg and body lengths directly measured by us from specimens. Yellow-shaded area indicates the range of body masses and leg lengths of small and medium sized Palearctic and Nearctic water striders that have typically been studied in the past. Blue-shaded area indicates body masses and leg lengths that have not been studied earlier. The data point for *A. paludum* is highlighted to indicate the largest of the species (belongs to Gerrinae) studied that uses surface-tension jump.

Supplementary Materials PART 2: Supplementary Movies

Description of the content of the supplementary video clips with the article:

Supplementary Movie 1 – ***Gigantometra gigas*** **jumping in the natural habitat and the water container and the bubble sheath around the leg.** Movie timeline: 1-3 s. – normal speed (1x); 4-10 s. – slowed down 8x; the clip shows two examples of upward jumps by the giant water strider and landing on the water surface (C0143). The water strider leaves the field of view in the video that was filmed at a closer distance (C0153). Movie timeline: 11-12 s. – normal speed (1x); 13-16 s. – slowed down 10x; the clip shows two examples of two different upward jumps by the giant water strider in the water container in the front (EVT16) and side view (EVT19). Movie timeline: 17-22 s. – slowed down 20x; the clip shows two examples around the leg of jumping water strider (EVT22 (2)) and dead leg striking into the water surface (C0143 dead leg).

Supplementary Movie 2 – ***Ptilomera tigrina*** **jumping in the water container and the bubble sheath around the leg.** Movie timeline: 1-3 s. – slowed down 4x; 4-6 s. – slowed down 16x; the clip shows two examples of two different upward jumps by the water strider in the water container in the front (C0046) and side view (C0049).

Supplementary Movie 3 – ***Aquarius paludum*** **jumping in the water container without breaking water surface.** Movie timeline: 1-3 s. – slowed down 4x; 4-6 s. – slowed down 20x; the clip shows an example of an upward jump by the water strider in the water container in the front (P_female_evt26) and side view (P_female_evt25).

Description of the content of the additional video clips available at Wikimedia and You tube (with links):

NATURAL HABITAT JUMP1.mp4. The clip shows an example of an upward jump by the giant water strider. The movements are slowed down (0.0375 normal speed). The second smaller water strider jumping belongs to the genus *Ptilomera*. *The movie (C0143) was captured in the field at 239.76fps and saved in the standard format of 29.97fps, which was additionally slowed down to 30% of playback speed.*
Wikimedia: https://commons.wikimedia.org/wiki/File:Gigantometra_gigas_upward_jump_in_Natural_Habitat_Pumat_National_Park_Jump_1.webm
Youtube: https://youtu.be/2EuG5vT4YHs

NATURAL HABITAT JUMP 2.mp4. The clip shows an example of an upward jump by the giant water strider. The movements are slowed down (0.125 normal speed). The giant water strider enters the field of view from the left. The smaller water strider on the right belongs to the genus *Ptilomera*. *The movie (C0153) was captured in the field at 239.76fps and saved in the standard format of 29.97fps, resulting in the slowdown of 0.125 relative to the normal speed.*
Wikimedia: https://commons.wikimedia.org/wiki/File:The_giant_water_strider_(Gigantometra_gigas;_Gerridae)_Natural_Habitat_Jump_2.webm
Youtube: https://youtu.be/jGN1gJBlk5k

NATURAL HABITAT JUMP3.mp4. The clip shows an example of an upward jump by the giant water strider. The movements are slowed down (0.0375 normal speed). The second smaller water strider jumping belongs to the genus *Ptilomera*. *The movie (C0027) was captured in the field at 479.52 fps and saved in the standard format of 29.97fps, resulting in the slowdown of 0.0625 relative to the normal speed.*
Wikimedia: https://commons.wikimedia.org/wiki/File:Gigantometra_gigas_(Gerridae)_Natural_Habitat_Jump_3.webm
Youtube: https://youtu.be/zyW-eV9kxs8

NATURAL HABITAT JUMP4.mp4. The clip shows an example of an upward jump by the giant water strider filmed at a closer distance. The water strider leaves the field of view. The movements are slowed down (0.125 normal speed). The giant water strider enters the field of view from the left. *The movie (C0148) was captured in the field at 239.76fps and saved in the standard format of 29.97fps, resulting in the slowdown of 0.125 relative to the normal speed.*
Wikimedia: https://commons.wikimedia.org/wiki/File:Gigantometra_gigas_(Gerridae)_Natural_Habitat_Jump_4.webm
Youtube: https://youtu.be/tCtFqlHHisU

NATURAL HABITAT JUMP5.mp4. The clip shows a close-up on the water surface under the water strider legs. The movements are slowed down (0.01875 normal speed). At the end of the clip, several small bubbles of air, which was originally wrapped around midlegs during the drag phase of the jump, "pop-up" on the water surface after being dis-attached from the legs (visible in the supplementary video "JUMP IN THE BOX.mp4"). *The movie (C0086) was captured in the field at 959.04 fps and saved in the format of 59.94 fps, which was additionally slowed down to 30%.*
Wikimedia: https://commons.wikimedia.org/wiki/File:Gigantometra_gigas_(Gerridae)_Natural_Habitat_Jump_5.webm
Youtube: https://youtu.be/bbwkCEwDtrA

JUMP IN THE TANK 1.AVI. The clip shows an example of an upward jump by the giant water strider filmed by Trouble Shooter camera (TS1000) with 500 fps. This is one of the three movies analyzed (*EVT16*).
Wikimedia: https://commons.wikimedia.org/wiki/File:Gigantometra_gigas_(Gerridae)_JUMP_IN_THE_TANK_1.webm
https://commons.wikimedia.org/wiki/File:Gigantometra_gigas_(Gerridae)_Jump_in_Tank_1_annotated_EVT16_50%25.webm
Youtube: https://youtu.be/wSd5EKYdPi8

JUMP IN THE TANK 2.mp4. This clip shows a close up of the midlegs moving downward and surrounded by air sheath caught in the hair around the leg. Eventually, the legs are quickly mowing upward and leave the air sheath, which forms air bubbles that travel slowly upwards towards the surface. This clip (*EVT22 (2) ind20*) was filmed by Trouble Shooter camera (TS1000) at 500 fps.
Wikimedia: https://commons.wikimedia.org/wiki/File:Gigantometra_gigas_(Gerridae)_JUMP_IN_THE_TANK_2_70PERC.webm
Youtube: https://youtu.be/ReE8NQhjo_4

JUMP IN THE TANK 3.mp4. This clip shows nearly symmetrical movements downwards of midlegs. The movements are slowed down (0.03125 normal speed). The air released from the legs under water creates small air bubbles that travel slowly upwards towards the surface. *The movie (C0041) was captured with Sony RX10-III at 959.04 fps and saved in the format of 59.94 fps, which was additionally slowed down to 50%.*
Wikimedia: https://commons.wikimedia.org/wiki/File:Gigantometra_gigas_(Gerridae)_JUMP_IN_THE_TANK_3.webm
Youtube: https://youtu.be/DagN4SMZOgc

JUMP IN THE TANK 4.mp4. This clip shows a close-up on legs seen approximately from the side to illustrate that during fast leg downward movements the air sheath (air bubble) around the legs is extended along the direction of leg movements (also seen in the two other clips: JUMP IN THE TANK 2 and DEAD LEG DOWNWARD MOVE. Therefore we could imagine that a crossection of leg including the air bubble may resemble an irregular ellipse rather than a circle. The drag force is proportional to the effective leg diameter, which is a function of the diameter of the leg plus the thickness of the air measured during downward movement in the plane perpendicular to the leg downward movement (see Supplementary Materials PART 7 for more details on how this aspect was simplified in the theoretical model). The movements are slowed down (0.015625 normal speed). *The movie (C0046) was captured with Sony RX10-III at 959.04 fps and saved in the format of 59.94 fps, which was additionally slowed down to 25%.*
Wikimedia: https://commons.wikimedia.org/wiki/File:Gigantometra_gigas_(Gerridae)_JUMP_IN_THE_TANK_4.webm
Youtube: https://youtu.be/DagN4SMZOgc

DEAD LEG DOWNWARD MOVE.mp4. This clip shows how midleg's hairs capture air during fast downward movements in the water. The movements are slowed down (0.03125 normal speed). *The movie (C0143) was captured in the field at 959.04 fps and saved in the format of 59.94 fps, which was additionally slowed down to 50%.*
Wikimedia: https://commons.wikimedia.org/wiki/File:Gigantometra_gigas_(Gerridae)_DEAD_LEG_DOWNWARD_MOVE.webm
Youtube: https://youtube.com/shorts/-f6E80VricM?feature=share

JUMPING OF *AQUARIUS PALUDUM*:
Near-vertical jumps of water strider (*A. paludum*) slow motion. - The video clip shows a slow motion of a water strider jumping upwards. Note the "dimples" under the legs and how they increase in depth while the legs push down and "bend" the water surface without breaking it. The model in *Nat Commun* **7,** 13698 (2016) https://doi.org/10.1038/ncomms13698 focuses on this ability of insects to jump upward without breaking of the water surface. It shows that this ability results in maximization of the jump speed and minimization of the latency between the jump initiation and leaving the water surface in the response to attacking predators.
Wikimedia: Water-striders-adjust-leg-movement-speed-to-optimize-takeoff-velocity-for-their-morphology-ncomms13698-s2.ogv
Youtube: https://youtu.be/8sjSmX5pNw8

Water strider *A. paludum* jump side view. - Slow motion video of the water strider Aquarius paludum jumping on the water surface. Side view reveals the backward leg movements. The speed is approximately 0.006 of normal speed.
Wikimedia: https://commons.wikimedia.org/wiki/File:Water_strider_A_paludum_jump_side_view.webm
Youtube: https://youtu.be/cDwGRyFiNoM

Waterstrider *A. paludum* jump frontal view. - Slow motion video of the water strider Aquarius paludum jumping on the water surface. Frontal view reveals the inward leg movements. The speed is approximately 0.006 of normal speed.
Wikimedia: https://commons.wikimedia.org/wiki/File:Waterstrider_A_paludum_jump_frontal_view.webm
Youtube: https://youtu.be/GLy7Obl6jLc

Water strider *A. paludum* jump on solid substrate. - This video of a water strider jumping on a solid substrate illustrates that the leg movements are composed of two phases. First phase comprises downward movement against the substrate surface (normally surface of water) dominates. The second phase comprises mostly horizontal movements: first backwards then inwards. When this happens on water, where each leg creates a dimple, the leg movements are associated with the dimple shifts backwards and then inwards. The speed is approximately 0.006 of normal speed.
Wikimedia: https://commons.wikimedia.org/wiki/File:Water_strider_A_paludum_jump_on_solid_substrate.webm
Youtube: https://youtu.be/4Sr0im-umSU

Supplementary Materials PART 3: Jumps of large-sized water striders

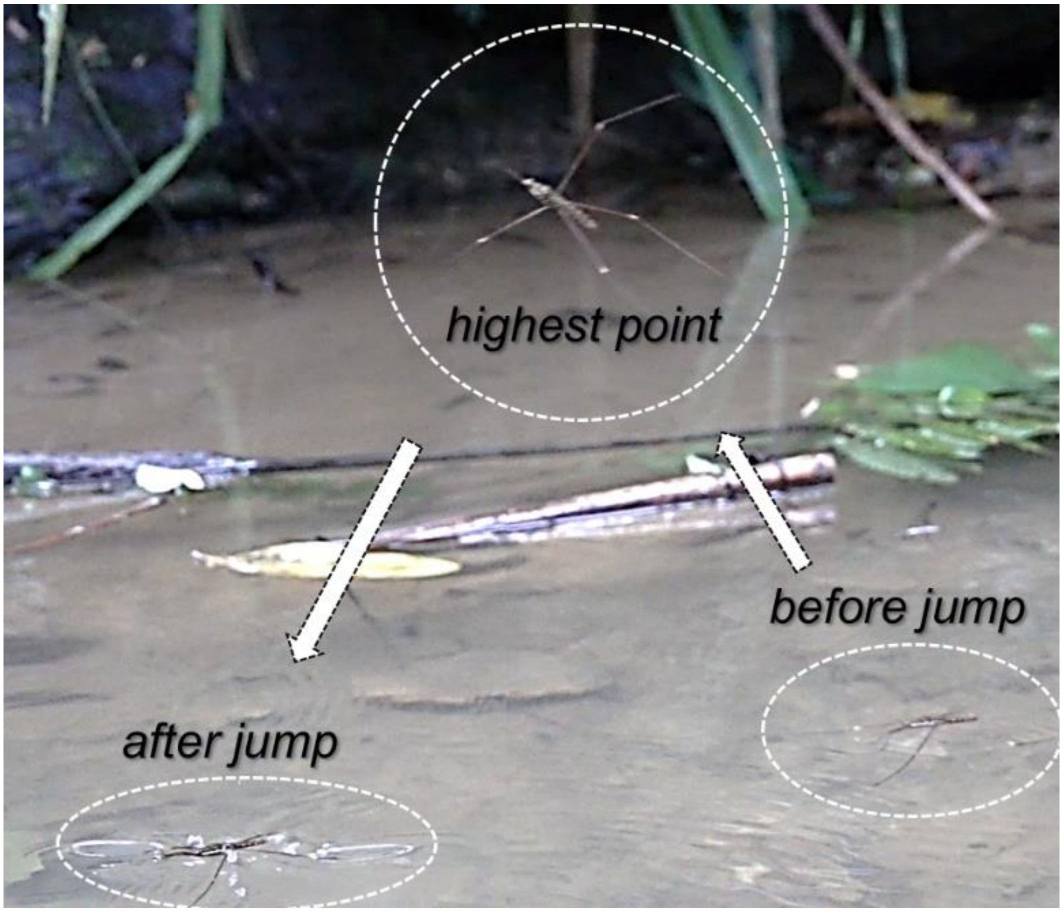

Fig. S2. Jumping in the natural habitat. An example of a record of one jump in the natural habitat. Three frames are put together here and photo-edited to represent the moment just before jump, the moment of reaching the highest point, and the moment right after landing on the water surface again. In the natural habitat, jumps of the giant water strider were triggered by imitating attacks from under the water surface using long bent sticks, or by creating a very fast visual stimulus by waving a sheet of paper in the visual field of the water strider. High speed movies were shot using Sony RX10-III. See details in Supplementary Movie 1.

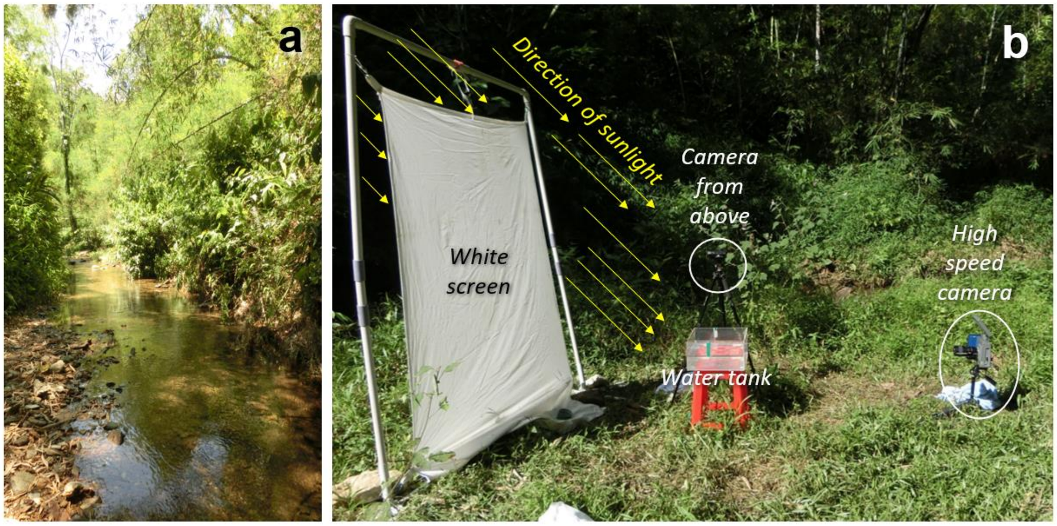

Fig. S3. Field methods. a) Study site in the natural habitat of the giant water strider in the Pumat National Park area. b) Experimental setup used in the field to obtain high-speed movies of jumping giant water striders. A water strider was put in a transparent water tank. Jumping was triggered by poking the insect gently from under water using a hook-shaped wire. Battery-operated high-speed camera (TS 1000) was used to film the jump, while standard camcorder filmed it from above to provide information about distance of the insect to the front wall of the tank (this distance was crucial to translate pixel coordinates into centimeters). A white sheet of fabric spread behind the water tank appropriately located with regard to the direction of sun light was used as a background. For some jumps, Sony RX10-III was used instead of the TS 1000.

In the water container, the slow-motion movies used for the detailed analyses have been shot using Trouble Shooter camera (TS 1000) set to film at 500 fps. The set-up is shown in Fig. S3. This setup requires two people for efficient work: one operates the high-speed camera, and the second person handles the water striders and triggers the jumps. Sometimes the water striders used their wings to escape from the water tank and these escapes were not analyzed.

Table S5. Observed number of Water surface breaking by midlegs of large-sized water striders: *G. gigas* and *P. tigrina*. Jumps without abnormal situation (e.g., insect exhausted and their leg was in the water) were counted. Breaking was defined as breaking with at least one leg by assuming that in asymmetric jumps the other has lighter load.

	G. gigas	*P. tigrina*	sum
Breaking occurred	57	21	78
No breaking	0	2	2
sum	57	23	80

Supplementary Materials PART 4: Duration of jump phases in *Gigantometra gigas*

Table S6. Duration of each phase of the jumps of *G. gigas* in the water container. "Surface tension phase" is from the start of the jump until surface breaking starts. "Transition phase" is from the start of surface breaking until the end of surface breaking. "Drag phase" is from the end of surface breaking until leg reaches the deepest point (i.e., leg stops moving downward). Bubble attached phase is from the start of surface breaking until the air sheath is completely detached from the leg and floats upwards in the form of bubbles. "After breaking phase" is from the start of surface breaking until leg reaches the deepest point (hence is it a sum of "Transition phase + Drag phase"). See also Figure S4 based on these data.

Video (leg)	Surface tension phase (ms)	Transition phase (ms)	Drag phase (ms)	Bubble attached phase (ms)	After breaking (ms)
EVT05 (2) left	22	12	16	32	28
EVT05 (2) right	30	10	12	10	22
EVT16 left	28	14	14	24	28
EVT16 right	26	8	14	36	22
EVT41 left	22	18	16	22	34
EVT41 right	12	14	32	28	46
EVT12	26	20	20	28	40
EVT14	26	10	16	22	26
EVT28	30	8	6	16	14
EVT33	24	14	12	20	26
EVT35	32	6	12	18	18
EVT45	28	6	18	28	24
EVT47	28	16	12	16	28
EVT65	44	4	12	18	16
EVT75	28	14	18	24	32
Mean (±s.d.)	**27.1 (±6.7)**	**11.6 (±4.7)**	**15.3 (±5.7)**	**22.8 (±6.8)**	**26.9 (±8.6)**

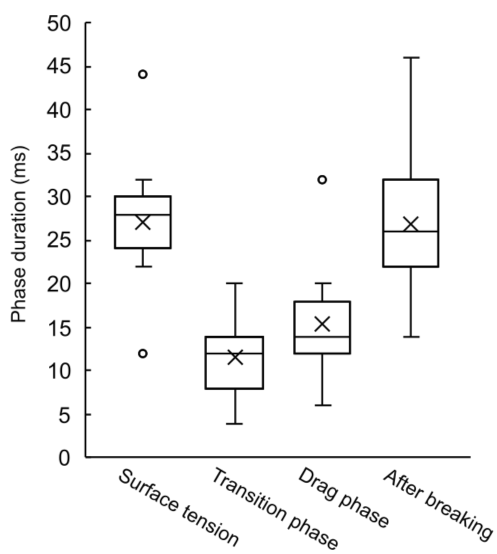

Fig. S4. Box-whisker plots of phase durations (ms). Duration of each phase of the jumps of *G. gigas* in the water container. Surface tension phase is from start of the jump until surface breaking starts. Transition phase is from the start of surface breaking until end of surface breaking. Drag phase is from end of surface breaking until leg reaches the deepest point (i.e., leg stops moving downward). Bubble attached phase is from the start of surface breaking until bubble detached from the leg. After breaking phase is from the start of surface breaking until leg reaches the deepest point. (hence it is a sum of "Transition phase + Drag phase"). The data are in Supplementary Table S6.

Supplementary Materials PART 5: Additional Results from the detailed analyses of jumps

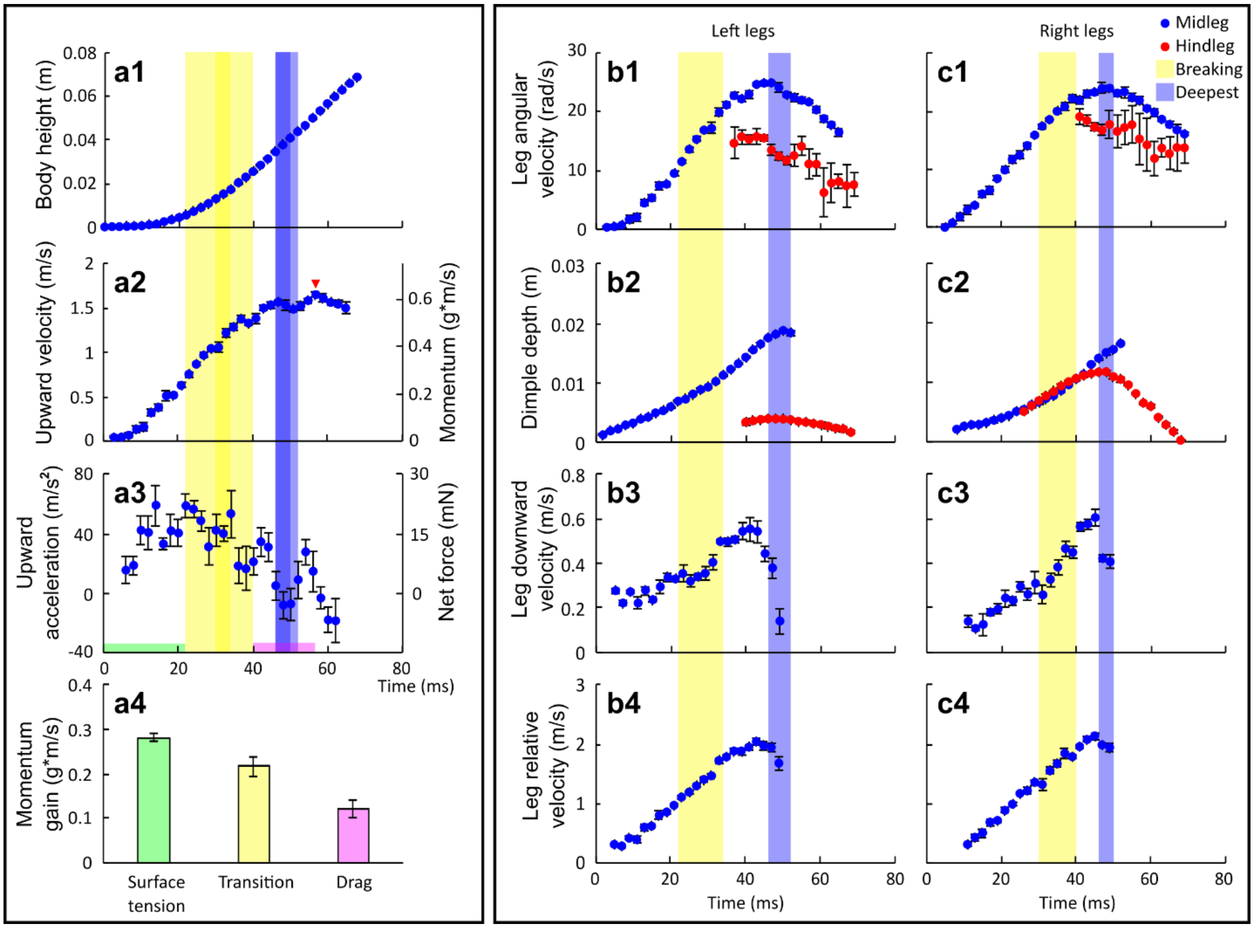

Fig. S5 Kinematics and dynamics of the jumping on water by the giant water strider, *Gigantometra gigas*. Results from analysis of a jump "EVT05 (2)". a) variables obtained from the body movement: changes of body height above the water surface (a1), body velocity (a2) and body acceleration (a3) during the jump. Right side axes in a2 and a3 indicated the changes of body momentum (a2) and net force (a3) during the jump calculated from the body movement and body mass. (a4) shows the comparison between the values of momentum gained during the three phases of jump: the surface tension phase (green), the transition phase (yellow) and the drag phase (purple). b) and c) contain variables concerning movements of the left (b) and right (c) midlegs (blue circles) and hindlegs (red circles in b1, b2, c1, c2): angular downward velocity (b1, c1), depth (b2, c2), downward velocity (b3, c3) and downward velocity relative to the body position (b4, c4). Yellow background indicates the transition phase when surface is breaking. Blue background indicates the bubble detaching phase duration of each leg. Red triangle in a2 indicates the moment of maximal body velocity.

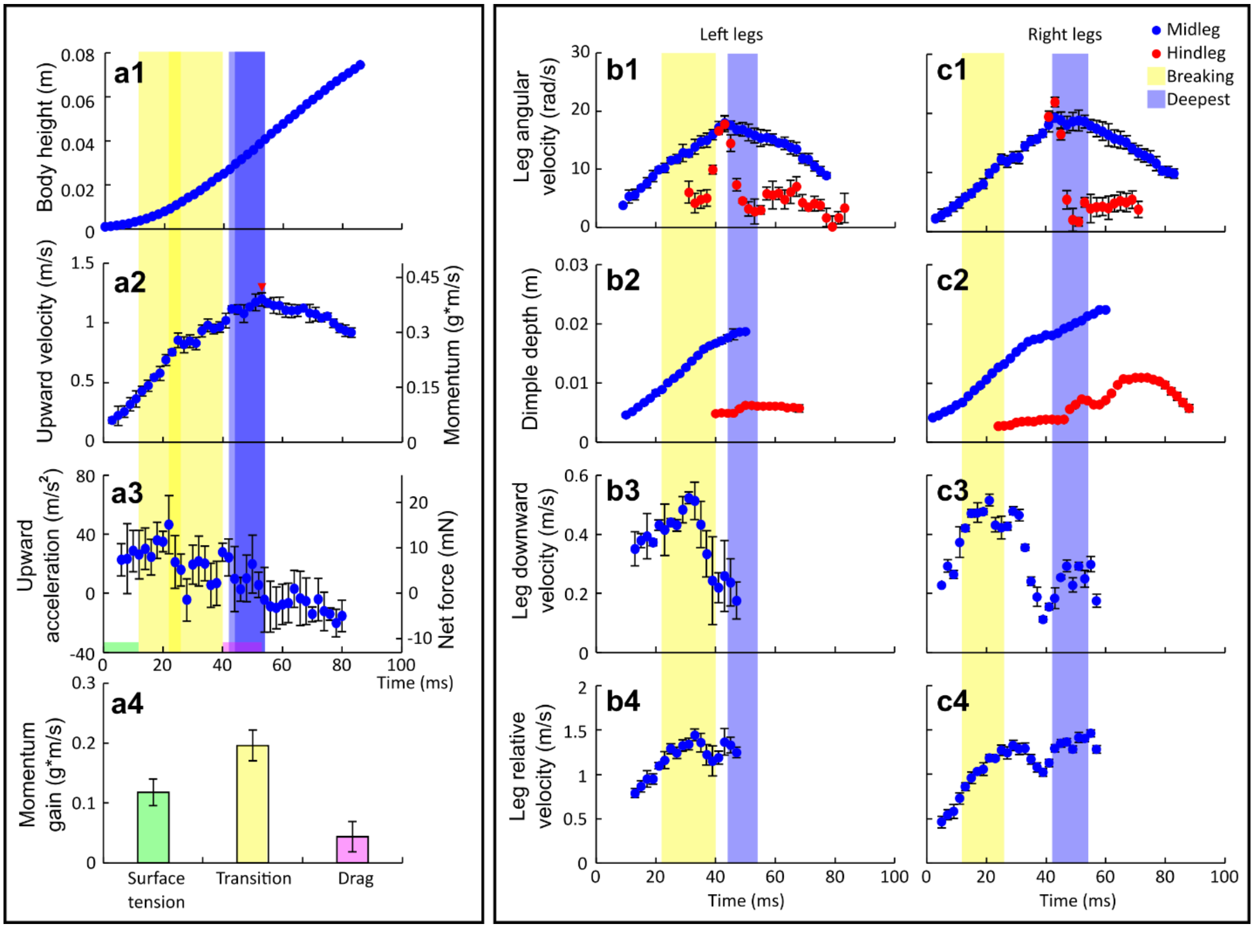

Fig. S6 Kinematics and dynamics of the jumping on water by the giant water strider, *Gigantometra gigas*. Results from analysis of a jump "EVT41". a) variables obtained from the body movement: changes of body height above the water surface (a1), body velocity (a2) and body acceleration (a3) during the jump. Right side axes in a2 and a3 indicated the changes of body momentum (a2) and net force (a3) during the jump calculated from the body movement and body mass. (a4) shows the comparison between the values of momentum gained during the three phases of jump: the surface tension phase (green), the transition phase (yellow) and the drag phase (purple). b) and c) contain variables concerning movements of the left (b) and right (c) midlegs (blue circles) and hindlegs (red circles in b1, b2, c1, c2): angular downward velocity (b1, c1), depth (b2, c2), downward velocity (b3, c3) and downward velocity relative to the body position (b4, c4). Yellow background indicates the transition phase when surface is breaking. Blue background indicates the bubble detaching phase duration of each leg. Red triangle in a2 indicates the moment of maximal body velocity.

Fig. 3 of the main text, and Fig. S5, S6 present the details extracted from the three best movies. In total we observed 65 jumps (51 in males and 14 in females) by 17 individuals (12 males and 5 females). We also recorded 43 jumps by 5 individuals of *Ptilomera tigrina*. In all observed jumps the water striders broke the water surface and the jump was produced by a mixture of two types of forces: surface tension followed by drag. In all 65 jumps the legs moving in the water were surrounded by the layer of air captured within the long hairs of tibia and tarsi. Also, in all jumps the midlegs moving upward eventually lost some of the air in the form of bubbles. In all jumps, we observed the three main phases: surface tension, transition, and drag phase. See table S6 and Fig. S4 for timing of each phase based on timing recorded in 15 leg movement events from 12 videos.

Supplementary Materials PART 6: Assumptions and methods of digitizing

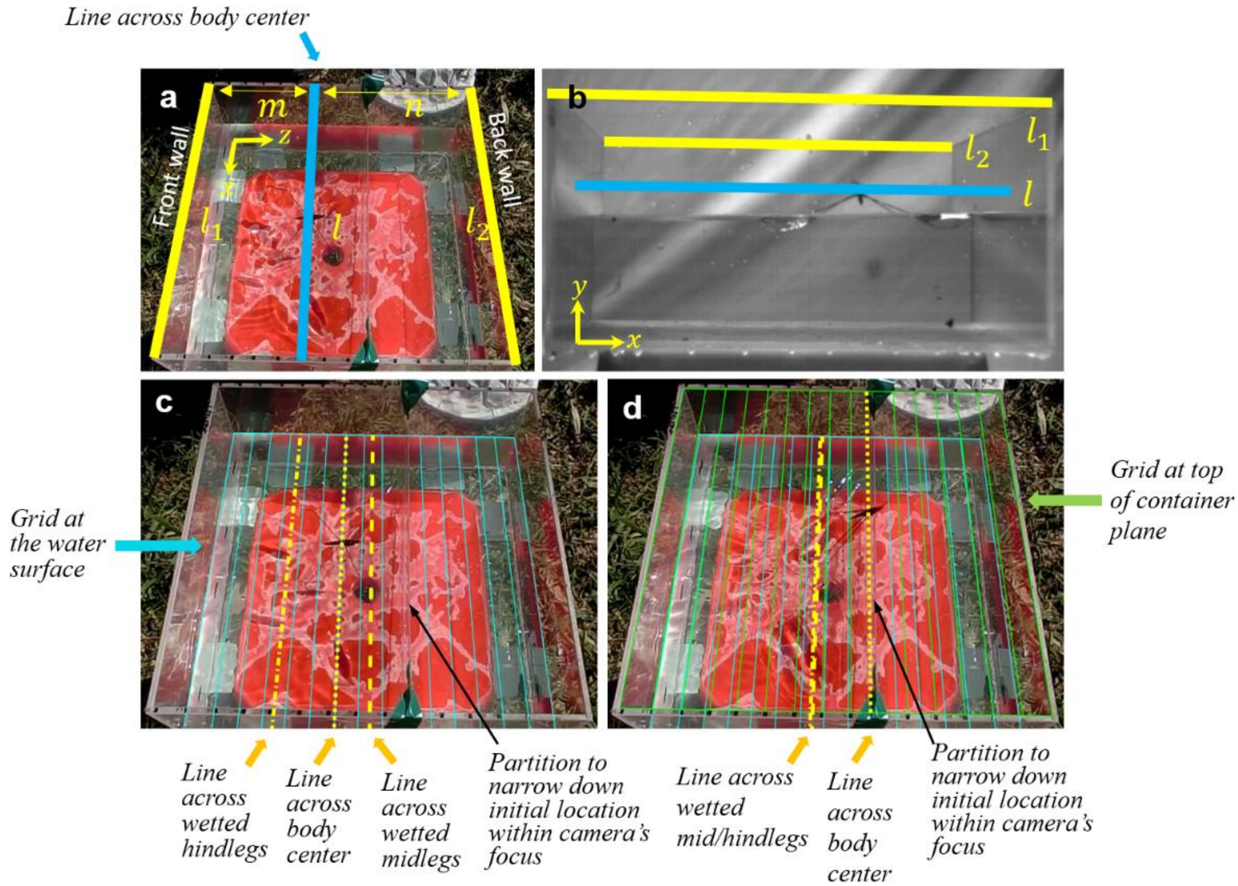

Fig. S7. The method of re-calculation from pixel-based to absolute (cm/mm) coordinates. High-speed camera recorded the jumping of the water strider through the front wall (left side wall in a) of the 30cm by 30cm transparent water tank, i.e., the high speed camera was facing the front wall marked with l_1, and its view is shown in b. The views in a, c, d are from a standard camcorder that recorded the jump from above. The thin blue lines at the level of water surface are 2cm apart. The real size of a pixel at any specific distance to the front wall (example of such a point is the water strider's body center through which a thick blue line crosses in a and b) was deduced from the following formula: $30cm/l = 30cm/(\frac{nl_1+ml_2}{m+n})$, where m and n are horizontal relative distances along the z-axis from the line across the digitized point (e.g., thick blue line across body center in a) to the front and back wall respectively, and l_1 and l_2 are lengths in pixels of the front and back wall in the view of the slow motion camera. This principle was directly applied to convert pixels to centimeters for the body center digitized (from the high-speed camera view) at the start of a jump (c) and at the takeoff (d). The body center z-axis at the takeoff was measured by using a grid in the plane corresponding to the upper part of the container (green lines), because the y axis coordinates of the body center at the takeoff were approaching this upper plane and were distant from the plane of the water surface (d). Hence for these two points of time, the m and n values were directly measured from an image from the standard camera view from above at two different planes: the water level plane for the start of jump (blue grid at the water surface) and the top-of-container plane for the takeoff moment (when legs still left on water surface; blue grid in c, d). The conversion from pixels to centimeters for frames located between these two points of time used m and n values calculated assuming a linear change of m (and n) during the jump duration between the initial (c; start of jump) and final (d; moment of takeoff) values of m and n. The same procedure was applied to the legs. For the two points digitized on legs (point of contact with water and the deepest point of tibia/tarsus for midlegs, as well as femur/tibia joint and the deepest point for hindlegs), we used an approximate distance to the front wall, m (and the corresponding distance to the back wall, n). It was approximately assumed to be the distance between the line going through the midrange of the wetted midleg/hindleg (marked as broken yellow lines in c, d).

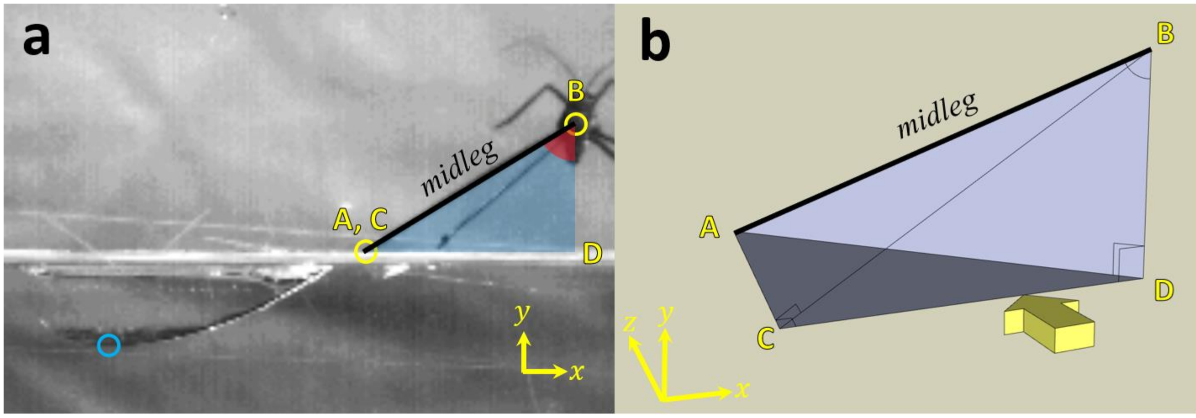

Fig. S8. **Calculations of midleg-to-vertical angles for each frame**. Points on the water surface (A, C), the deepest point (blue circle) of the middle leg, and the body center (B) were tracked in every frame using MaxTRAQ program. The vertical angle of a midleg (ABD) was defined as angle between section AB (along the leg) and vertical line (section BD). However, the camera (3D arrow along the lens's axis indicates the direction to where the camera was pointing) provided direct measure of distances and angles within the plane marked by the triangle CBD (i.e., plane perpendicular to the lens axis). Using this information together with the inferred distance AB (from insect empirical measurements of leg length and proportion of leg above water measured from the video) we estimated (by trigonometry) the angle ABD in each frame in movies with insects facing the camera while jumping. The formulas are explained below:

The angle between the midleg (section AB) and the vertical line (red shaded angle in Fig. S8a; angle ABD in b) was calculated in each frame using the trigonometric functions and coordinates of the body center and the water surface contact point of the middle leg. The middle leg angle is expressed as below.

$$\angle\text{Middle leg} = \angle\text{ABD} = \tan^{-1}\frac{\overline{AD}}{\overline{BD}} = \tan^{-1}\frac{(\overline{AC}^2 + \overline{CD}^2)^{1/2}}{\overline{BD}}$$

$$= \tan^{-1}\frac{\sqrt{(Body_z - Surface_z)^2 + (Body_x - Surface_x)^2}}{Body_y - Surface_y}$$

$$= \tan^{-1}\frac{\sqrt{(B_z - A_z)^2 + (B_x - A_x)^2}}{B_y - A_y}$$

The angle between the hind leg's femur and the vertical line was calculated in each frame by the three-dimensional approximation using the second law of the cosines and using the known length of femur (Fig S9). The angle was calculated as below.

$$\angle\text{Hind leg} = \angle\text{ABD} = \cos^{-1}\left(\frac{\overline{AB}^2 + \overline{BD}^2 - \overline{AD}^2}{2\cdot\overline{AB}\cdot\overline{BD}}\right)$$

$$= \cos^{-1}\left(\frac{\overline{AB}^2 + \overline{BD}^2 - (\overline{AC}^2 + \overline{CD}^2)}{2\cdot\overline{AB}\cdot\overline{BD}}\right)$$

$$= \cos^{-1}\left(\frac{\overline{AB}^2 + \overline{BD}^2 - [(\overline{AB}^2 - \overline{BC}^2) + \overline{CD}^2]}{2\cdot\overline{AB}\cdot\overline{BD}}\right)$$

$$= \cos^{-1}\left(\frac{\overline{BD}^2 + \overline{BC}^2 - \overline{CD}^2}{2\cdot\overline{AB}\cdot\overline{BD}}\right)$$

$$= \cos^{-1}\left(\frac{(B_y - D_y)^2 + \left[\left(B_y - C_y\right)^2 + (B_x - C_x)^2\right] - (D_x - C_x)^2}{2 \cdot \overline{AB} \cdot (B_y - D_y)}\right)$$

$$= \cos^{-1}\left(\frac{(B_y - C_y)^2 + \left[\left(B_y - C_y\right)^2 + (B_x - C_x)^2\right] - (B_x - C_x)^2}{2 \cdot \overline{AB} \cdot (B_y - C_y)}\right)$$

$$= \cos^{-1}\left(\frac{B_y - C_y}{\overline{AB}}\right)$$

The angle was calculated since the length of the femur ($\overline{AB}$) was already known from empirical measurements.

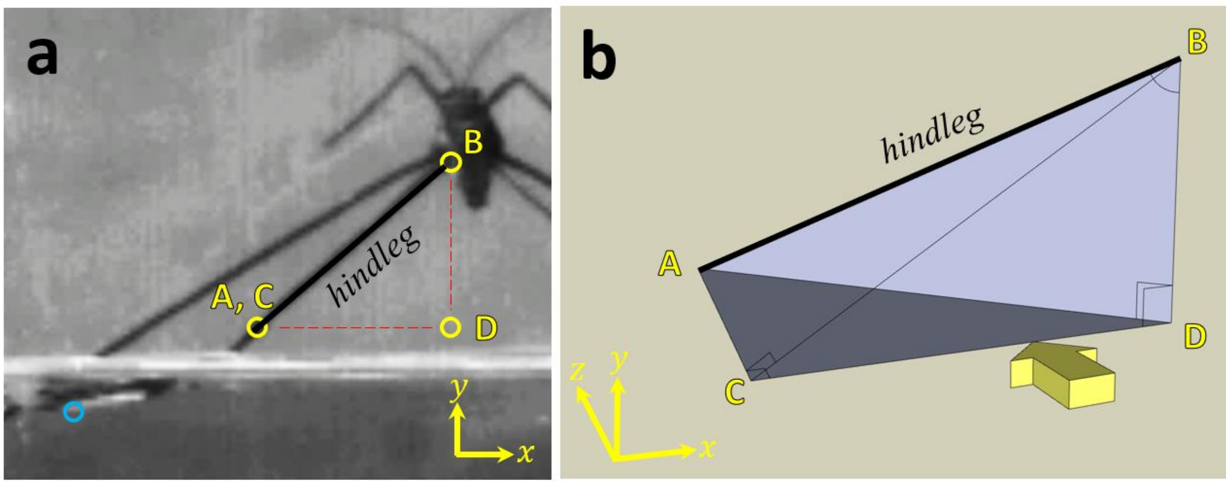

Fig. S9. **Calculations of hindleg-to-vertical angles for each frame**. Hind femur angle was calculated for each frame from the empirically measured femur length and information extracted from the video. As we knew the real femur length of the hind leg ($\overline{AB}$), the angle $\angle ABD = \cos^{-1}(\frac{B_y - C_y}{\overline{AB}})$. Femur tip (yellow) and the deepest point (blue) of the hind leg were also digitized.

Supplementary Materials PART 7: Extraction of information from empirical measurements for the model's assumptions about the functional/effective diameter of the wetted leg.

The model dramatically simplifies some of the aspects of reality. One of the simplifications is an assumption about midleg shape that is used to estimate the drag force in the drag phase of a jump. The model assumes that the two midlegs are cylinders of a diameter based on the empirical measurements of legs of water striders and on the empirical estimates of the air volume captured around the leg during a jump. The functional (effectively working for drag force) leg diameter during the initial moments of the drag phase, when air sheath surrounds the leg, is calculated assuming that the air surrounds the cylinder as a uniform layer (Fig. 10d) of a thickness calculated from the empirically derived measurements of the volume of air caught around the leg (Table S7).

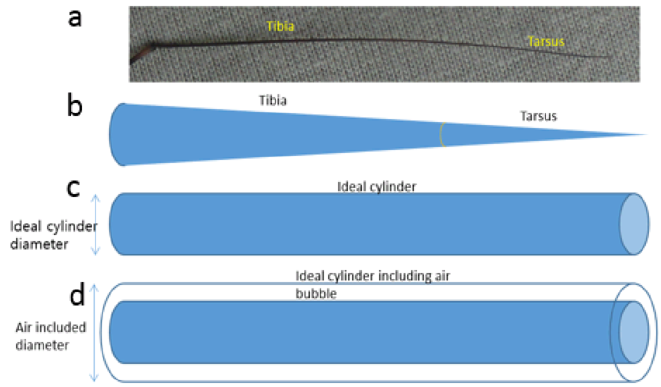

Fig. 10. Tibia and tarsus of the real water strider leg (a) considered for calculations. At the first approximation, tibia and tarsus were assumed to form an ideal cone (b) of the length of the total length of tibia and tarsi, and the diameter ranging from the thickness of the proximal tibia at the femur/tibia joint to zero (at the tip). At the next step of approximation, we assumed the leg is a cylinder with the diameter (ideal cylinder's volume in (c) equal to the volume of the cone in (b)). Air-including radius was calculated by assuming that the volume of the air bubble covered the ideal cylinder evenly (d): i.e., knowing the physical length and diameter of an ideal cylinder-shaped wetted leg (c), we estimated the thickness of the air assuming that air surrounds the leg in a uniform symmetrical manner (d).

Table S7. Calculated ideal radius of a cylinder imitating the midleg, and the ideal radius of a cylinder imitating the midleg surrounded by air (air sheath/air bubble)

Video name	EVT16	EVT05 (2)	EVT41	Mean (SE)
Ideal radius (mm)	0.131	0.113	0.137	0.127 (0.07)
Bubble volume for a leg (mm^3)	43.4	9.90	36.3	29.9 (10.2)
Air included radius (mm)	0.520	0.285	0.482	0.429 (0.73)
Radius ratio with/without air bubble	3.96	2.54	3.52	3.34 (0.42)

The model assumes that the radius of leg cylinder imitating the leg with the air sheath around it is 3.34 times as large as the radius of cylinder imitating the leg without the air sheath. This ratio was assumed in all model simulations, even when it was applied to smaller species with less developed leg hairs that may capture air. Therefore, the modeled performance of the hypothetical drag-involving jumps by the smaller species is slightly overestimated, and we mention this in Discussion. Nevertheless, despite this overestimation the hypothetical drag –involving jumps by the smaller species did not generally show higher performance than surface tension jumps of these species.

Supplementary Materials PART 8: Observations of hindlegs in the jumps of *Gigantometra gigas*.

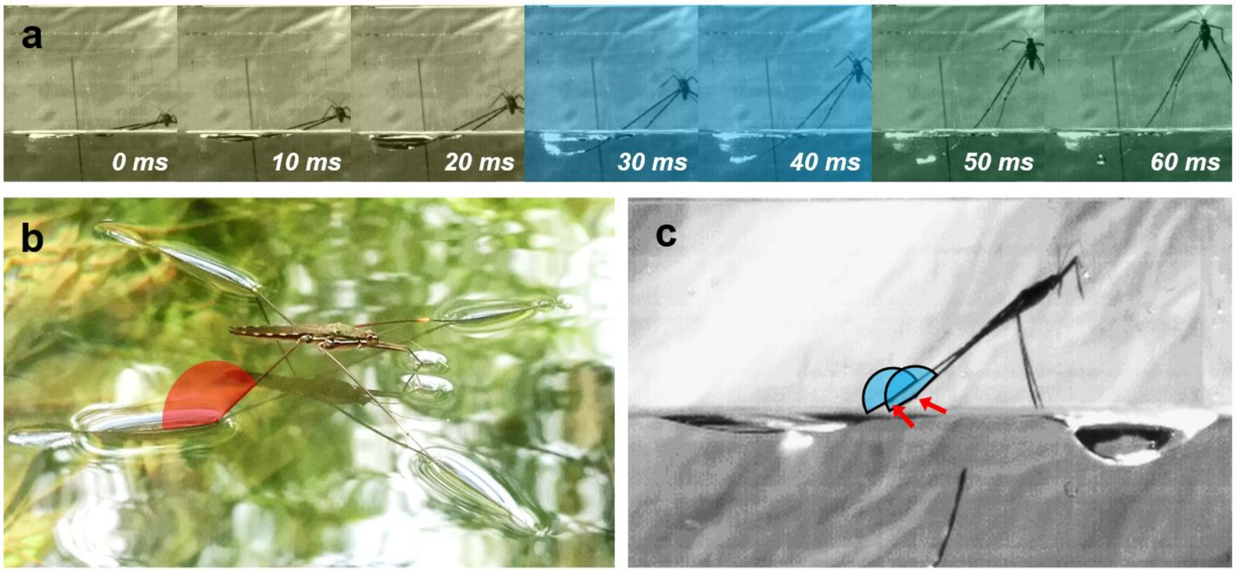

Fig. S11. Hindlegs in the jump of the giant water strider. Changes of body pitch during the jump analyzed in Fig. 3 are the most pronounced in the final phase (40-60 ms in a), when a sudden short-lasting increase in the downward angular velocity of hindlegs occurs (in Fig. 3, S5, S6). Hindleg's dimples depth remain relatively stable at the initial phases (0-20 ms of surface tension phase in a) and subsequently during the transition and drag phases (30-40 ms in a), and they are generally similar to the dimples in resting position (b). During the jump, the angle between femur and tibia at the femur/tibia joint appears to remain roughly similar for extensive portion of the jump. The resulting dimples during jump may deepen slightly in the final stages of jump when the body pitch changes, and when the femur/tibia angle (marked red) becomes wider and approaches 180^o in the final stages of the hindlegs' leaving the water surface. However, this typically this does not lead to breaking the water surface (a, c) because the hindlegs bend quite extensively (c) and because the water strider's legs at this stage are already moving upwards and do not push the surface (green shaded frames in a). Red arrows in (c) mark the femur-tibia joints for each hindlegs.

Supplementary Materials PART 9: Hindleg's constant depth, h_{hm}.

To calculate for each movie and species the theoretically assumed constant depth of a hindleg (h_{hm}; see page 4 in Supplementary Model Descripion), we used empirical maximum depth from high-speed videos. The constant depth used in the model (h_{hm}) was calculated from the empirical maximum depth, h_{hE}, and wetted leg length, l_h, assuming the wetted length as a half of an arc. The average depth of the arc was used as the constant depth.

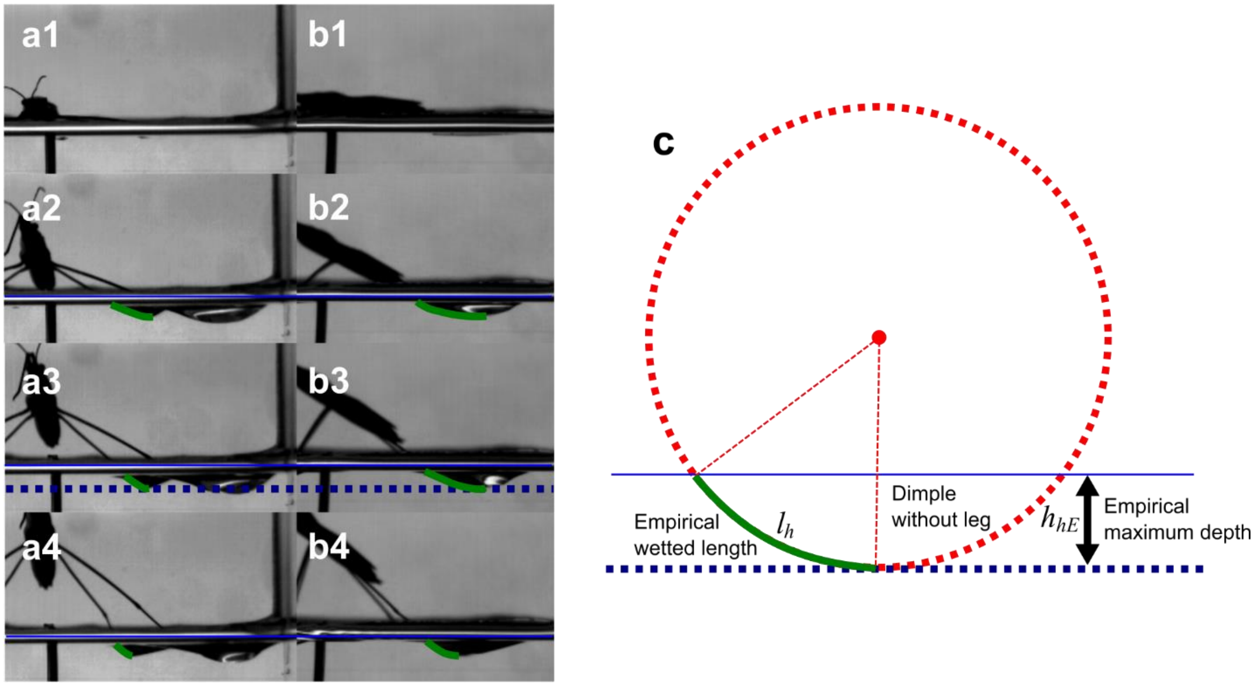

Fig. S12. The constant depth of hind leg. The constant depth, $\boldsymbol{h_{hm}}$, was calculated as an average depth of a half of an arc that has same maximum depth, $\boldsymbol{h_{hE}}$ and wetted length, $\boldsymbol{l_h}$, of empirical measurements of species.

Supplementary Materials PART 10: Maximum jumping height calculation.

If an object takes off vertically at the moment of takeoff, t_f, with the takeoff velocity, v_f, from initial height, H_0, object will be at the maximum height, H_m, when the total kinetic energy transferred to potential energy. Hence, the maximum jumping height, H_m, can be calculated as follows:

$$E_{potential} = mgh = mg(H_m - H_0) = E_{kinetic} = \frac{1}{2}mv_f^2$$

$$H_m = H_0 + \frac{v_f^2}{2g}$$

Supplementary Materials PART 11: Additional empirical results for *G. gigas* females and *P. tigrina*

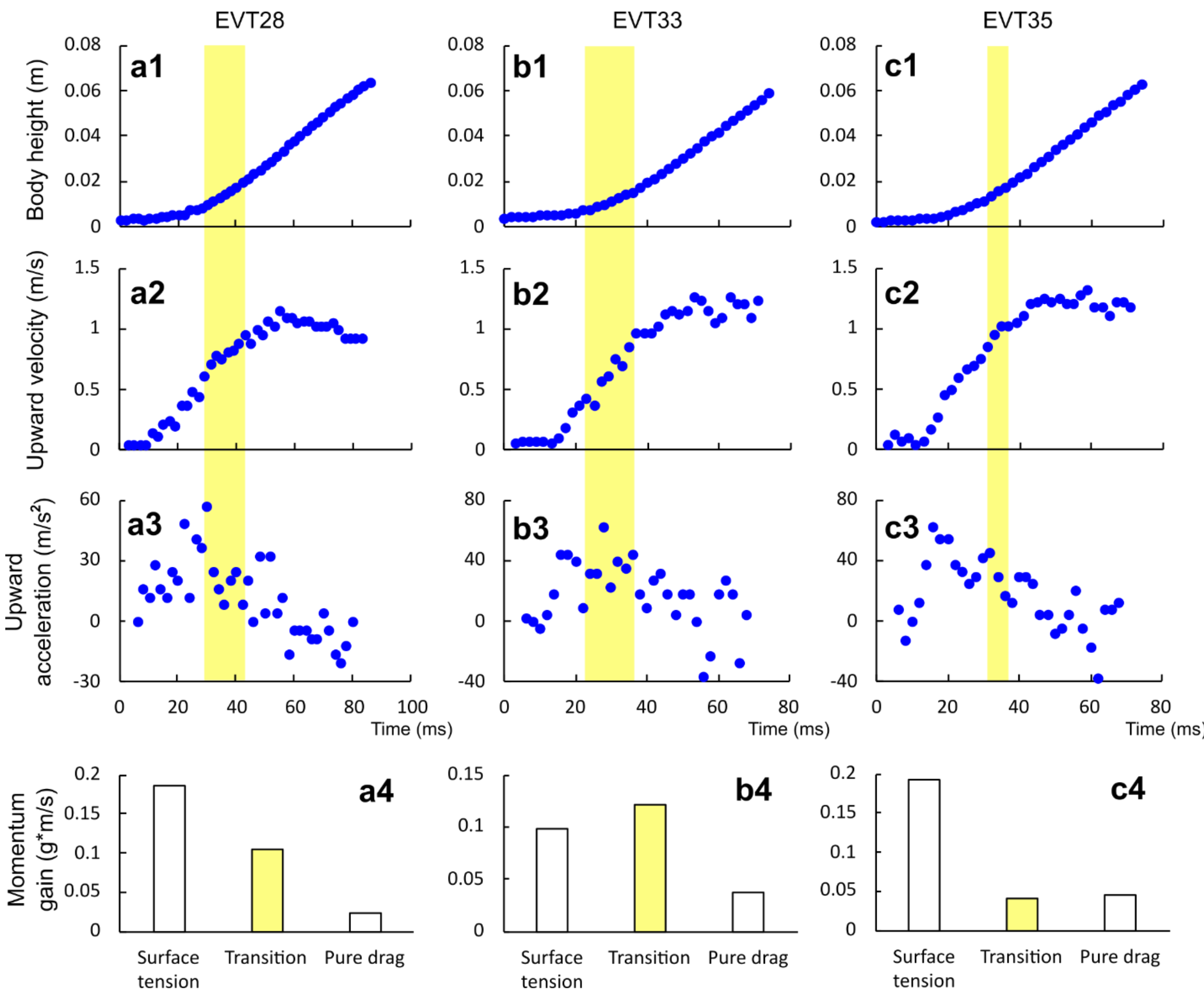

Fig. S13. Kinematics of the jumping on water by the giant water strider (*Gigantometra gigas*) females. Extra results from analyses of jumps "EVT28", "EVT33", "EVT35". a1, b1, c1 show body height; a2, b2, c2 show body velocity; a3, b3, c3 show body acceleration during the jump. a4, b4, c4 show the comparison between the values of momentum gained during the three phases of jump: the surface tension phase, the transition phase (yellow), and the drag phase. The vertical yellow band across the panels indicates the transition phase when surface is in the process of breaking.

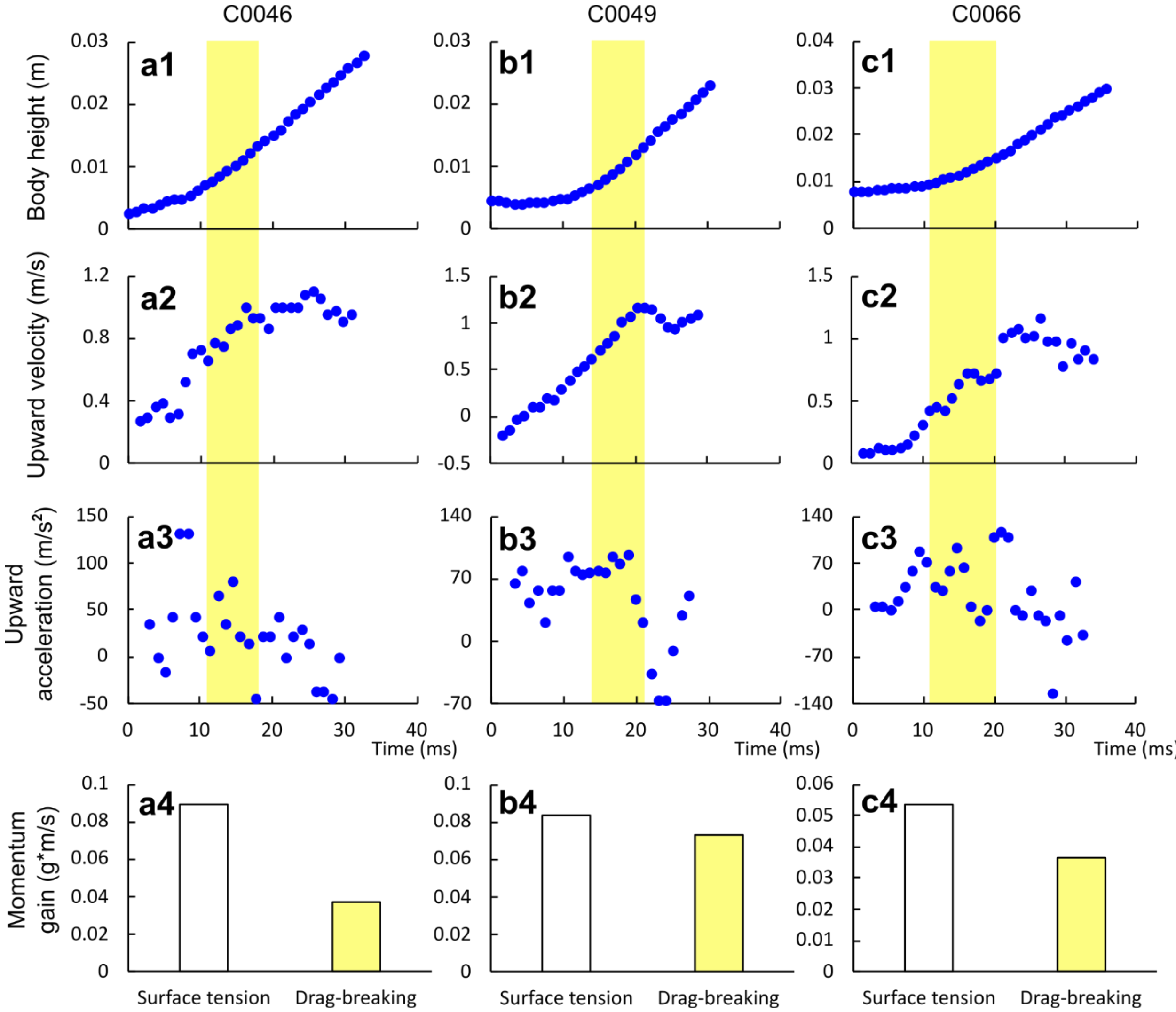

Fig. S14. Kinematics of the jumping on water by *Ptilomera tigrina*. Results of analysis of jumps in movies "C0046", "C0049", "C0066". a1, b1, c1 show body height; a2, b2, c2 show body velocity; a3, b3, c3 show body acceleration during the jump. a4, b4, c4 show the comparison between the values of momentum gained during the two phases of jump: the surface tension phase, and the drag-breaking phase (corresponding to the transitional phase in *G. gigas)*. Pure drag phase is not observed because *P. tigrina* legs go up before full breaking of the middle leg dimple. Yellow vertical bands across the panels indicates the "drag-breaking" phase (i.e., the transition phase) when surface is in the process of breaking under the midlegs (see also Supplementary Movie 3).

Supplementary Materials PART 12: Model validation - comparison with empirical observations

Extra results are similar to those shown in Fig. 3 in the main text. The results illustrate a reasonable match between empirical (Data from Supplementary Materials PART 11) and theoretical trajectories of body center for specific jumps of three females of *G. gigas* (Fig. S15 a-c) and three individuals of *P. tigrina* (Fig. S15 d-f).

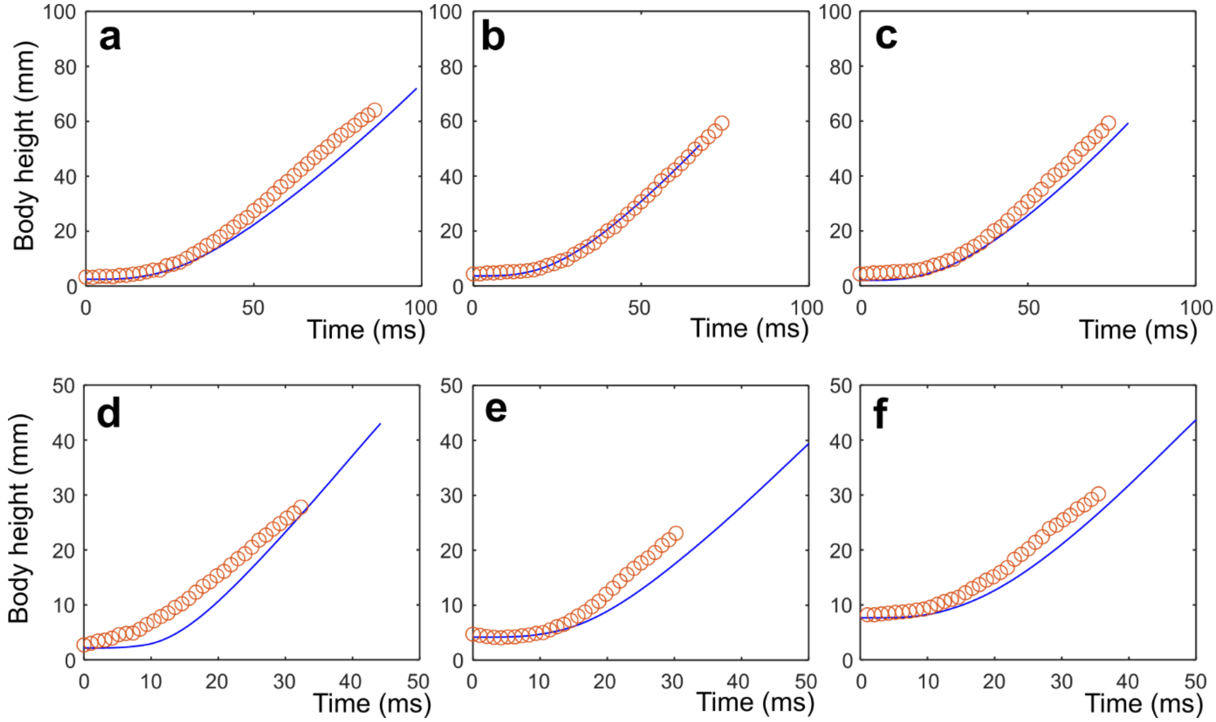

Fig. S15. The model results (simulations of separate jumps based on empirically measured input into the model) compared to the empirically observed trajectories for individual jumps of *G. gigas* females and *P. tigrina*. (a, b, c) - The theoretical model results and empirical results for the jumps of *G. gigas* females in movies EVT28, EVT33, and EVT35. (d, e, f) - The theoretical model results and empirical results for the jump videos of *P. tigrina*: C0046, C0049, and C0066. Horizontal axis represents time (ms); Vertical axis represents height of body center above water surface (mm). Blue line indicates model results and orange circles represent empirically measured values

Supplementary Materials PART 13: Validation of the use of empirical constant angular velocity of the middle leg rotation, ω_e.

One of the model's simplifying assumptions is that the angular downward midleg movement occurs at a constant angular velocity that can be determined from empirical data on leg and body coordinates from the videos under certain assumptions described in Yang et al.[2], where it was shown to be acceptably close to the empirical average of angular velocity and resulted in valid conclusions regarding the surface tension jumps in small and medium size water striders[1]. This angular velocity of middle leg rotation, ω_e, is empirically derived from basic observations of jump kinematics under the assumption that the empirically measured linear downward velocity of wetted midleg relative to water surface, v_l, can be approximated by the simple formula: $v_l = \omega(l_l - y_i)sin(2\omega t) - \dot{y}$, while the vertical distance from the tip of the legs to the body center, l_s, can be approximated by another formula: $l_s = \Delta l[1 - \frac{1}{2}\cos(2\omega t) + y_i]$ (see Yang et al.[2] and Supplementary Model Description for more details). To validate our use of the same procedure for determining the simple value of constant angular velocity of middle leg rotation, ω_e, we compared the empirically observed leg movements in specific jumps where in reality the leg angular velocity of rotation vary during a jump with the theoretical leg movements calculated using the constant value of ω_e extracted from each video separately. We did this for 3 jumps from each size category: *G. gigas* male, *G. gigas* female, and *P. tigrina* (data from Fig. 3, S13, S14, S15). The results suggest an approximate reasonable agreement between observed and theoretically predicted profiles of leg tip distance to body and leg tip relative velocity during jumps performed by relatively synchronized symmetrical movements by the left and right midleg.

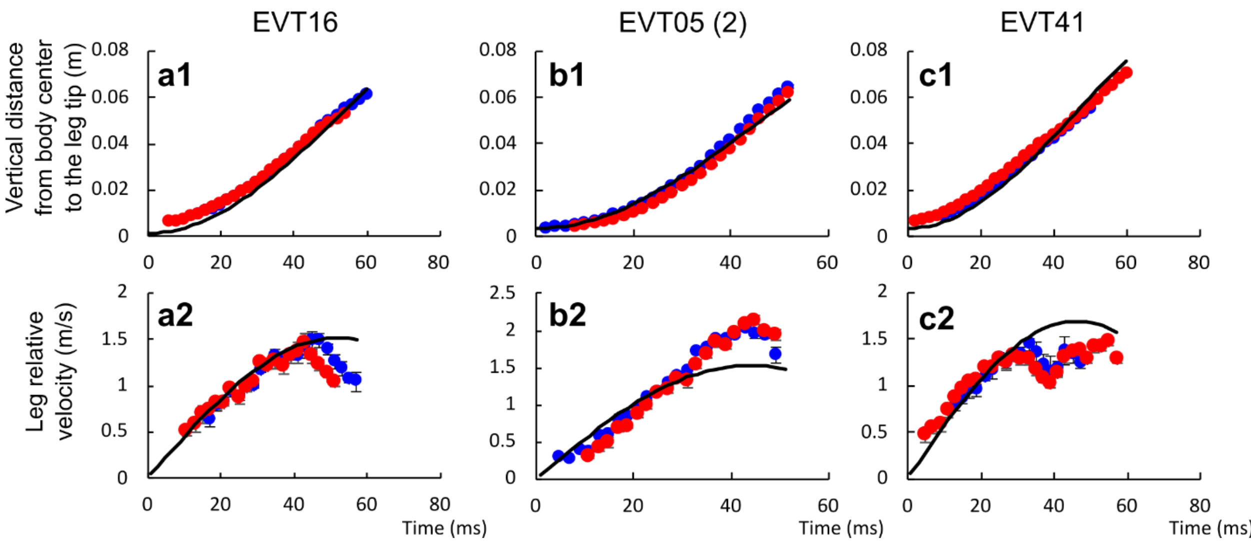

Fig. S16. Comparison of the theoretical predictions based on constant midleg angular velocity, ω_e, with the observations of water striders (*G. gigas* males), who naturally use midleg angular velocity that varies during the course of a jump. (a1, b1, c1) – The profile of the vertical distance from body center to the leg tip in jumps by *G. gigas* males; (a2, b2, c2) - The profile of the velocity of the leg relative to the body center in jumps of *G. gigas* males. Data from videos EVT16 (a1, a2), EVT05 (2) (b1, b2), and EVT41 (c1, c2). Red dots indicate left leg and blue dots indicate right leg. We also extracted the values of constant empirical angular velocity of leg rotation, $\boldsymbol{\omega_e}$[2] in these jumps in order to use the values in Fig. 5, 6 as the indicators of the range of values of midleg angular velocity by this species.

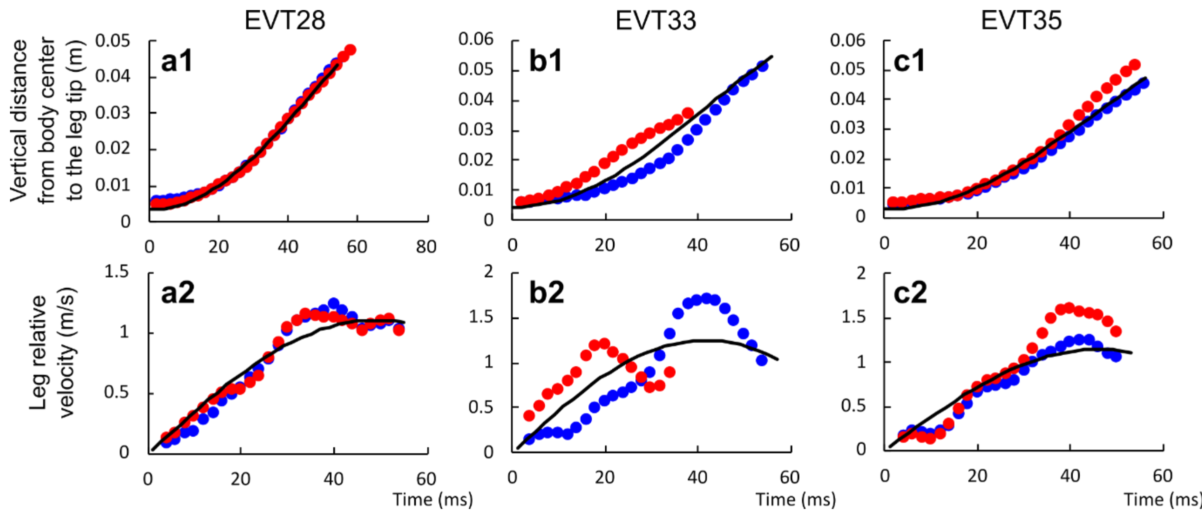

Fig. S17. Comparison of the theoretical predictions based on constant midleg angular velocity, ω_e, with the observations of water striders (*G. gigas* females), who naturally use midleg angular velocity that varies during the course of a jump. (a1, b1, c1) – The profile of the vertical distance from body center to the leg tip in jumps by *G. gigas* females; (a2, b2, c2) - The profile of the velocity of the leg relative to the body center in jumps of *G. gigas* females. Data from videos EVT28 (a1, a2), EVT33 (b1, b2), and EVT35 (c1, c2). Red dots indicate left leg and blue dots indicate right leg. We also extracted the values of constant empirical angular velocity of leg rotation, $\boldsymbol{\omega_e}^2$ in these jumps in order to use the values in Fig. 5, 6 as the indicators of the range of values of midleg angular velocity by this species.

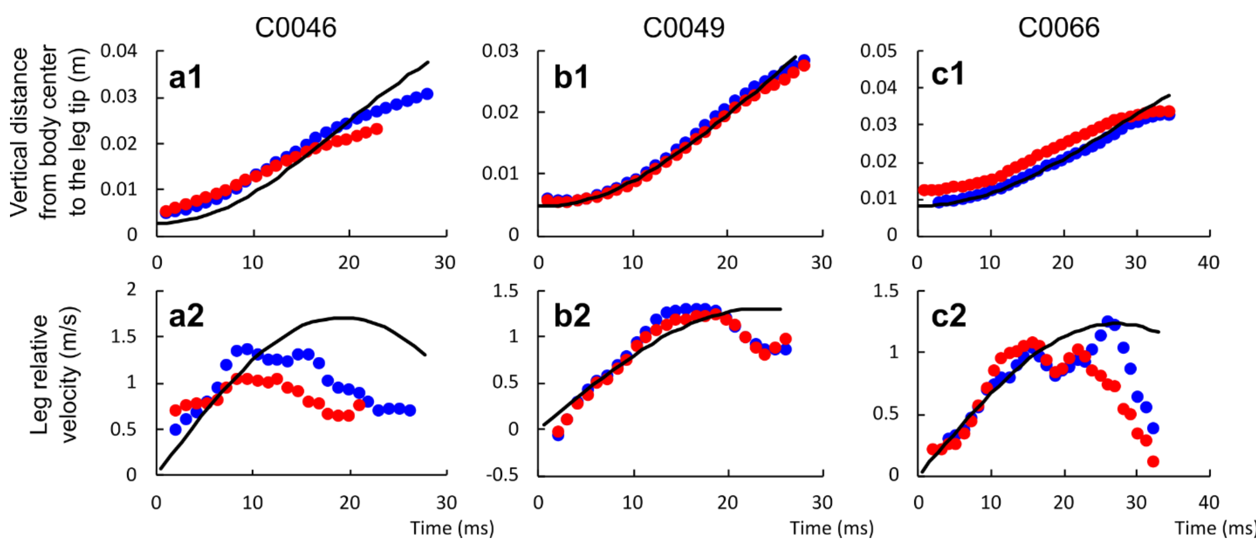

Fig. S18. Comparison of the theoretical predictions based on constant midleg angular velocity, ω_e, with the observations of water striders (*P. tigrina*), who naturally use midleg angular velocity that varies during the course of a jump. (a1, b1, c1) – The profile of the vertical distance from body center to the leg tip in jumps by *G. gigas* males; (a2, b2, c2) - The profile of the velocity of the leg relative to the body center in jumps of *G. gigas* males. Data from videos C0046 (a1, a2), C0049 (b1, b2), and C0066 (c1, c2). Red dots indicate left leg and blue dots indicate right leg. We also extracted the values of constant empirical angular velocity of leg rotation, $\boldsymbol{\omega_e}^2$ in these jumps in order to use the values in Fig. 5, 6 as the indicators of the range of values of midleg angular velocity by this species.

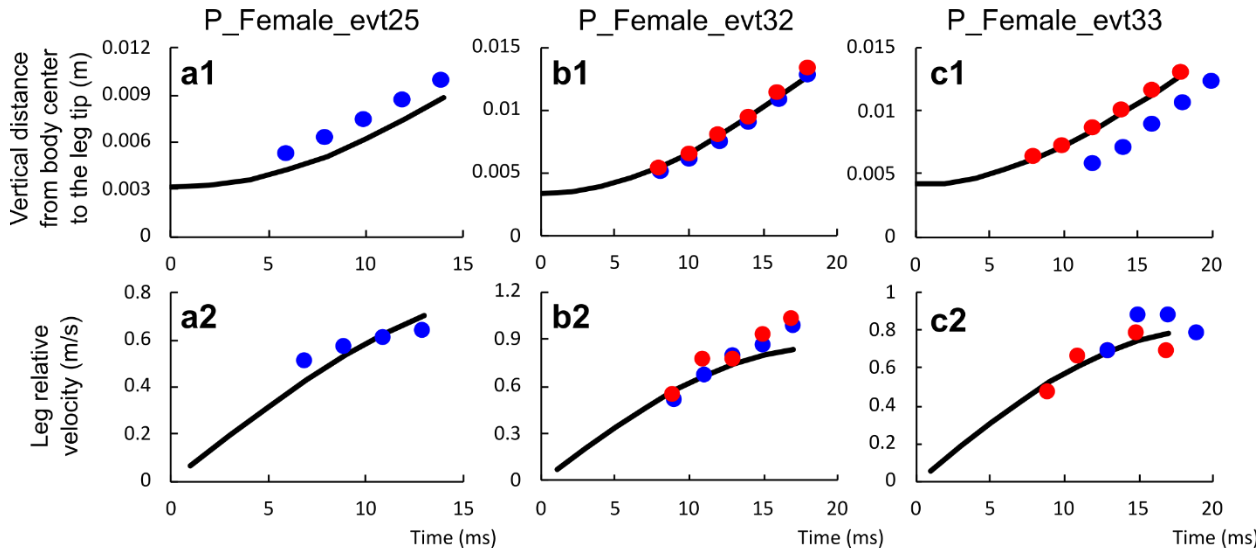

Fig. S19. Comparison of the theoretical predictions based on constant midleg angular velocity, ω_e , with the observations of water striders (*A. paludum* females), who naturally use midleg angular velocity that varies during the course of a jump. (a1, b1, c1) – The profile of the vertical distance from body center to the leg tip in jumps by *G. gigas* males; (a2, b2, c2) - The profile of the velocity of the leg relative to the body center in jumps of *G. gigas* males. Data from videos P_Female_evt25 (a1, a2), P_Female_evt32 (b1, b2), and P_Female_evt33 (c1, c2). Red dots indicate left leg and blue dots indicate right leg. We also extracted the values of constant empirical angular velocity of leg rotation, $\boldsymbol{\omega_e}^2$ in these jumps in order to use the values in Fig. 5, 6 as the indicators of the range of values of midleg angular velocity by this species. Only one leg was digitized in P_Female_evt25 since the other was not visible.

Supplementary Materials PART 14: Maximum jumping performance of fish.

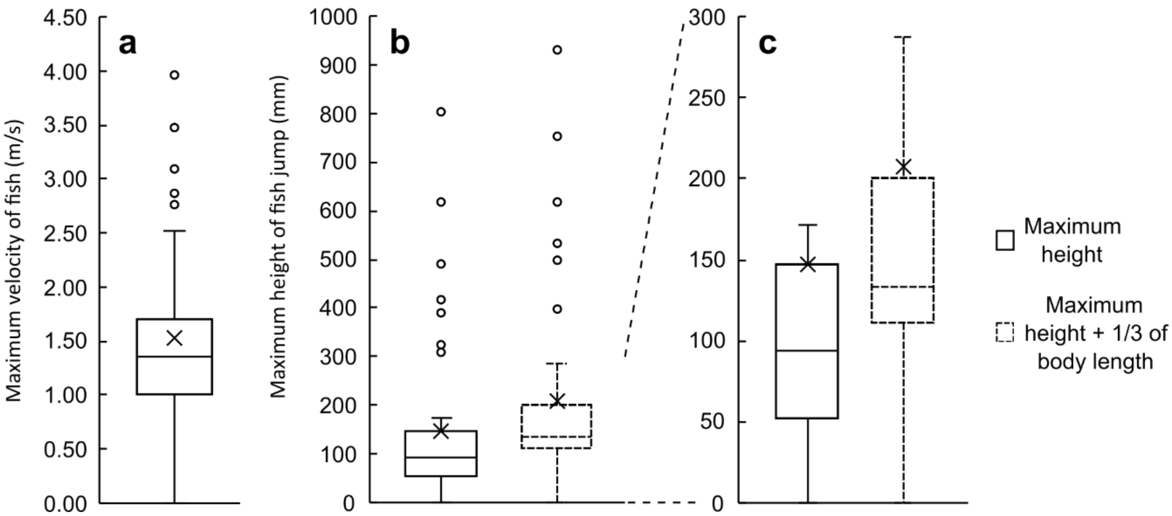

Fig. S20. The calculated hypothetical maximum performance of fish based on the literature on fish movement speeds[3]. a) Maximum velocity achieved by fish in the water; b, c) the estimated hypothetical height of jumping fish assuming that a fish of a given body length moves vertically upward with the body velocity recorded in the literature (shown in a) and calculated according to the formula explained in Supplementary Materials PART 10). The height from the water surface is represented by solid lines. The height including 1/3 of body length is represented by dashed lines by assuming fish lose their thrust when 1/3 of their body came out from the water.

References

1. Matsuda, R. Morphology, evolution and a classification of the Gerridae (Hemiptera-Heteroptera). *Univ. Kansas Sci. Bull.* **41**, 25–632 (1960).

2. Yang, E., Son, J. H., Lee, S. -i., Jablonski, P. G. & Kim, H.-Y. Water striders adjust leg movement speed to optimize takeoff velocity for their morphology. *Nat. Commun.* **7**, (2016).

3. Domenici, P. & Blake, R. W. The kinematics and performance of fish fast-start swimming. *J. Exp. Biol.* **200**, 1165–1178 (1997).